MOLECULAR AND CELLULAR BIOLOGY, July 2001, p. 4188–4196 Vol. 21, No. 13
0270-7306/01/$04.00+0 DOI: 10.1128/MCB.21.13.4188–4196.2001

Impaired Activity of the Extraneuronal Monoamine Transporter System Known as Uptake-2 in *Orct3*/*Slc22a3*-Deficient Mice

RONALD ZWART,[1] SANDRA VERHAAGH,[1] MARIJE BUITELAAR,[1] CORRIE POPP-SNIJDERS,[2] AND DENISE P. BARLOW[1]*

Department of Molecular Genetics (H5), The Netherlands Cancer Institute, 1066 CX Amsterdam,[1] and Department of Endocrinology, Free University, 1007 MB Amsterdam,[2] The Netherlands

Received 23 February 2001/Returned for modification 15 March 2001/Accepted 13 April 2001

Two uptake systems that control the extracellular concentrations of released monoamine neurotransmitters such as noradrenaline and adrenaline have been described. Uptake-1 is present at presynaptic nerve endings, whereas uptake-2 is extraneuronal and has been identified in myocardium and vascular and nonvascular smooth muscle cells. The gene encoding the uptake-2 transporter has recently been identified in humans (*EMT*), rats (*OCT3*), and mice (*Orct3*/*Slc22a3*). To generate an in vivo model for uptake-2, we have inactivated the mouse *Orct3* gene. Homozygous mutant mice are viable and fertile with no obvious physiological defect and also show no significant imbalance of noradrenaline or dopamine. However, *Orct3*-null mice show an impaired uptake-2 activity as measured by accumulation of intravenously administered [^{3}H]MPP$^+$ (1-methyl-4-phenylpyridinium). A 72% reduction in MPP$^+$ levels was measured in hearts of both male and female *Orct3* mutant mice. No significant differences between wild-type and mutant mice were found in any other adult organ or in plasma. When [^{3}H]MPP$^+$ was injected into pregnant females, a threefold-reduced MPP$^+$ accumulation was observed in homozygous mutant embryos but not in their placentas or amniotic fluid. These data show that *Orct3* is the principal component for uptake-2 function in the adult heart and identify the placenta as a novel site of action of uptake-2 that acts at the fetoplacental interface.

The catecholamines adrenaline, noradrenaline, dopamine, and the tryptophan derivative serotonin function as neurotransmitters of the monoaminergic neurons and as hormones in the control of physiological processes like glucose storage and metabolism, thermoregulation, and blood pressure. Changes in synaptic concentration or temporary availability of monoamines are associated with mental dysfunction, neuropsychiatric disorders, and drug addiction (10). Furthermore, altered plasma concentrations can result in physiological dysfunction (28). Tight control of the levels of synaptic and circulating catecholamines is thus essential for proper neuronal signaling and maintenance of internal homeostasis.

Two uptake systems that clear extracellular monoamines have been described. The neuronal uptake-1 system is present at presynaptic nerve endings and mediates the reuptake of released monoamines from the synaptic cleft. Uptake-1 is a high-affinity and Na^+- and Cl^--dependent system mediated by the noradrenaline (Net), dopamine (Dat), and serotonin (Sert) transporter proteins (reviewed in reference 1). Targeted inactivation experiments with mice have shown that the uptake-1 transporter proteins are a target for antidepressant and psychostimulatory treatments and are pivotal in the control of synaptic catecholamine concentrations and prevention of neurobehavioral changes (3, 14, 37).

The extraneuronal uptake-2 system was originally discovered in myocardial cells of the rat heart but has also been identified in vascular and nonvascular smooth muscle cells like those in the uterus, as well as in human central nervous system glial and kidney carcinoma cell lines (19, 24, 26, 31, 33). Uptake-2 can be discriminated from uptake-1 in substrate specificity and transport kinetics (reviewed in reference 33). In addition, corticosteroids, β-haloalkylamines, and O-methylated catecholamines are inhibitors of uptake-2 but not of uptake-1. The cyanine derivative disprocynium 24 (D24) was isolated as a highly potent uptake-2 inhibitor in vitro (23). However, the application of D24 in vivo to study uptake-2 was revealed to be limited, as it was shown previously that D24 blocks not only uptake-2 but also other transport mechanisms that clear catecholamines (8, 11).

Recently, molecular identification of the uptake-2 transporter protein has been reported. Called extraneuronal monoamine transporter (EMT) in humans and organic cation transporter 3 (OCT3) in rats, the protein is predicted to contain a 12-transmembrane domain structure (18, 36). The mouse homolog of the *EMT* and *OCT3* genes, called *Orct3* (locus name *Slc22a3*), was isolated from the critical region of the natural embryonic lethal mouse mutant t^{w73} and shown to be tightly linked to the closely related *Orct1*/*Slc22a1* and *Orct2*/*Slc22a2* organic cation transporter genes (35). This physical linkage is conserved in humans and suggests that these genes have evolved from a common ancestor. Further evidence for this comes from in vitro studies in which it has been shown that the Orct1, Orct2, and Orct3 proteins can all transport catecholamines and the neurotoxin MPP$^+$ (1-methyl-4-phenylpyridinium) (4, 16–18). However, transport inhibition studies have shown that only Orct3 is sensitive to all uptake-2 antagonists, including *O*-methylisoprenaline, with nearly identical kinetics (15, 18). In mice, the *Orct1*, *Orct2*, and *Orct3* genes have clearly distinct expression profiles. *Orct1* is expressed in liver, kidney, and intestine, whereas *Orct2* expression is restricted to the kidney and brain (21, 27). In contrast, *Orct3* expression is seen in a wide range of tissues. The highest

* Corresponding author. Present address: ÖAW Institute of Molecular Biology, Billrothstrasse 11, A-5020 Salzburg, Austria. Phone: 43 662 63 961 14. Fax: 43 662 63 961 40. E-mail: dbarlow@imb.oeaw.ac.at.

levels of expression are found in skeletal muscle and in the heart and uterus, for which uptake-2 activity has been described previously (33, 35). Similarly, high expression of the human homolog is found in aorta, prostate, adrenal gland, skeletal muscle, and liver (35). During mouse embryonic development, *Orct3* is expressed in the early postimplantation embryo (38). At later stages, expression is restricted to the labyrinth layer of the placenta, in which *Orct3* is coexpressed with the gene for the monoamine oxidase A (*Maoa*) metabolizing enzyme (34). Thus, both the in vitro studies and the expression data have provided strong evidence that *Orct3* is the molecular component of the extraneuronal monoamine transport (uptake-2) system.

To test whether *Orct3* has a major role in uptake-2 activity in any particular organ in vivo, we have generated mice deficient for *Orct3* by homologous recombination in embryonic stem (ES) cells. These mice are viable and fertile and show no obvious physiological defect and no significant imbalance of two tested monoamines, noradrenaline and dopamine. However, using MPP^+ as a substrate, we show that *Orct3* is an essential component for uptake-2 function in the adult heart and placenta but not in other adult organs. These data establish the presence of uptake-2 in the heart and identify the placenta as a novel uptake-2 site of action, where it functions at the fetoplacental interface.

MATERIALS AND METHODS

***Orct3* gene targeting.** For constructing the targeting vector, a 17.5-kb *Bgl*II fragment spanning the first exon of the mouse *Orct3* gene was isolated from the genomic BAC clone 228C21 (Research Genetics, Inc.) (35). To generate plasmid p16*Bgl*II, a 1.4-kb fragment from the 3′ end of the subclone was removed using *Asp*718, followed by religation. In p16*Bgl*II, a 4.3-kb *Bam*HI fragment containing exon 1, and 0.65 kb of upstream and 2.9 kb of downstream genomic sequences, was replaced by the pGKneo/pGKtk selection cassette flanked by loxP sites (9). The targeting vector was linearized with *Xho*I, and 50 μg was used in an electroporation of E14 (129/Ola) mouse ES cells. One hundred ninety-two individual colonies were screened for homologous recombination by hybridization with an 0.8-kb *Asp*718-*Spe*I 3′ external probe of *Bgl*II-digested genomic DNA. Six homologous recombinant clones were identified (i.e., a 3% recombination frequency). The integrity of the homologous recombination event was verified with a *Sal*I-*Bgl*II 5′ external probe in an *Spe*I digest (data not shown). The subclonal appearance of the targeted allele is caused by a contamination of the clones with surviving nontargeted ES cells (Fig. 1B). Four individually targeted ES cell clones were transiently transfected with a CRE expression plasmid to remove the neomycin/tk selection cassette. Individual clones were picked and analyzed for CRE-mediated recombination. Upon karyotyping, two independently derived ES cell clones with the *Orct3* (positive or negative) genotype were used for blastocyst injections to generate chimeric mice. Both clones resulted in germ line transmission and yielded similar results. The mutant *Orct3* allele was bred into an FVB/N genetic background for analysis and is available for distribution.

Genomic Southern blot analysis. ES cell genomic DNA was isolated by proteinase K digestion (100 μg/ml) in 100 mM Tris (pH 8.0)–5 mM EDTA–200 mM NaCl–0.2% sodium dodecyl sulfate. Five micrograms of DNA was used for digestion and run on a 0.6% agarose gel. Upon transfer of the DNA to a Hybond-N^+ nylon membrane (Amersham), hybridization was performed under Church hybridization conditions (6).

Northern blot analysis. Total RNA of mouse tissues was isolated by the lithium chloride extraction method (2). Analysis of the RNAs by Northern blotting was done as described previously (35). The *Orct3* probe was a 2.7-kb fragment from the 3′ end of the *Orct3* cDNA; mouse *Pai-1* and human glyceraldehyde-3-phosphate dehydrogenase (GAPDH) cDNAs were used as probes for loading control.

MPP^+ transport studies. The mice used for the time curve were 7-week-old wild-type FVB/N female mice. Four mice were injected for the 5- and 10-min points, and three mice were injected for the 15- and 60-min points. For the adult transport experiment, homozygous mutant *Orct3* or wild-type littermates of a mixed genetic background (25% 129/Ola, 75% FVB/N) were injected at the age of 12 weeks. Seven mice of each genotype were used. Timed matings were performed for the placental transport studies. Three pregnant mothers were injected at 15.5 days postcoitum (dpc) of gestation, resulting in a total of eight wild-type and six mutant embryos. [^{3}H]MPP^+ (methyl-4-phenylpyridinium acetate, *N*-methyl-^{3}H labeled, 77.5 Ci/mmol) was obtained from NEN Life Science Products, Inc., and was diluted 1:150 with cold MPP^+ iodide (Research Biochemicals International) to a final concentration of 0.2 mg/ml in 0.9% NaCl. After anesthesia with methoxyflurane (Medical Developments), animals were injected intravenously in the tail vein with 1.0 mg of the drug per kg of body weight. The mice were killed at the indicated time points by axillary bleeding after renewed anesthesia. Plasma and organs were collected, weighed, and frozen till further processing. Intestinal contents were separated from intestinal tissues. For the placental transport studies, placentas, embryos, and amniotic fluid as well as maternal blood were collected. Tissues were homogenized in 4% bovine serum albumin, and concentrations of [^{3}H]MPP^+-derived radioactivity were measured by liquid scintillation counting.

Statistical analysis. All values are given as means ± standard deviations (SD). The two-tailed unpaired Student *t* test was used to assess the significance of differences between data sets. Differences were considered to be statistically significant when P was <0.01.

Orct3 antiserum. Three polyclonal antibodies were raised in rabbits: (i) one against a C-terminal peptide at amino acids 524 to 542, synthesized onto a lysine tree; (ii) one against a fusion protein consisting of the large extracellular loop between TM1 and TM2 fused to maltose binding protein; and (iii) one against a similar fusion protein, which contained the large intracellular loop between TM6 and TM7. These regions are the least conserved among the *Orct1, Orct2,* and *Orct3* family members. Only the first antigen gave an antiserum which recognized the Orct3 protein in lysates from cells transfected with the wild-type *Orct3* gene in a Western blot assay. However, this antiserum was unable to detect Orct3 in placental or adult organ lysates. The *Orct3* gene is heavily glycosylated in vivo, and Western blotting produces bands only if transfected cells are treated with tunicamycin (5 μg/ml).

HPLC analysis of noradrenaline and dopamine. E12.5 embryos and placentas with a wild-type genotype and an *Orct3*-null genotype were obtained from heterozygous matings. The samples were prepared as described previously (32). Noradrenaline and dopamine concentrations were measured by high-performance liquid chromatography (HPLC) (Gynkotec; Separations) with electrochemical detection (Antec Leyden) using 3,4-dihydroxybenzylamine as an internal standard. Protein concentrations were determined as described previously (32), and noradrenaline and dopamine concentrations were expressed per milligram of protein.

RESULTS

***Orct3* gene targeting.** To inactivate the *Orct3* gene, a two-step targeting approach was used. First, a 4.3-kb genomic *Bam*HI fragment that contains the complete first exon of the *Orct3* gene and 650 bp of upstream sequences was replaced with a pGKneo/pGKtk selection cassette flanked by loxP sites (Fig. 1A). Successful homologous recombination was monitored by Southern blotting with a 3′ external probe, detecting a 17-kb wild-type (+/+) *Bgl*II fragment and a 9.5-kb fragment of the recombined allele (+/neo [Fig. 1B]). Subsequently, four independently targeted clones were transiently transfected with a CRE-recombinase expression vector to remove the pGKneo/pGKtk selection cassette. CRE-mediated recombination resulted in an *Orct3* knockout allele (+/−) that could be identified as a 12-kb *Bgl*II fragment (Fig. 1C). Thus, the resulting *Orct3* knockout allele lacked exon 1 and contained a single *loxP* site replacing a 4.3-kb genomic *Bam*HI fragment (Fig. 1A).

Two independently targeted and CRE-recombined ES cell clones were used for blastocyst injections to generate chimeric mice, and both ES clones passed through the germ line.

The Orct3 targeted allele is a complete null. It was anticipated that removal of the first exon and 650 bp of upstream sequences would result in the complete absence of *Orct3* gene

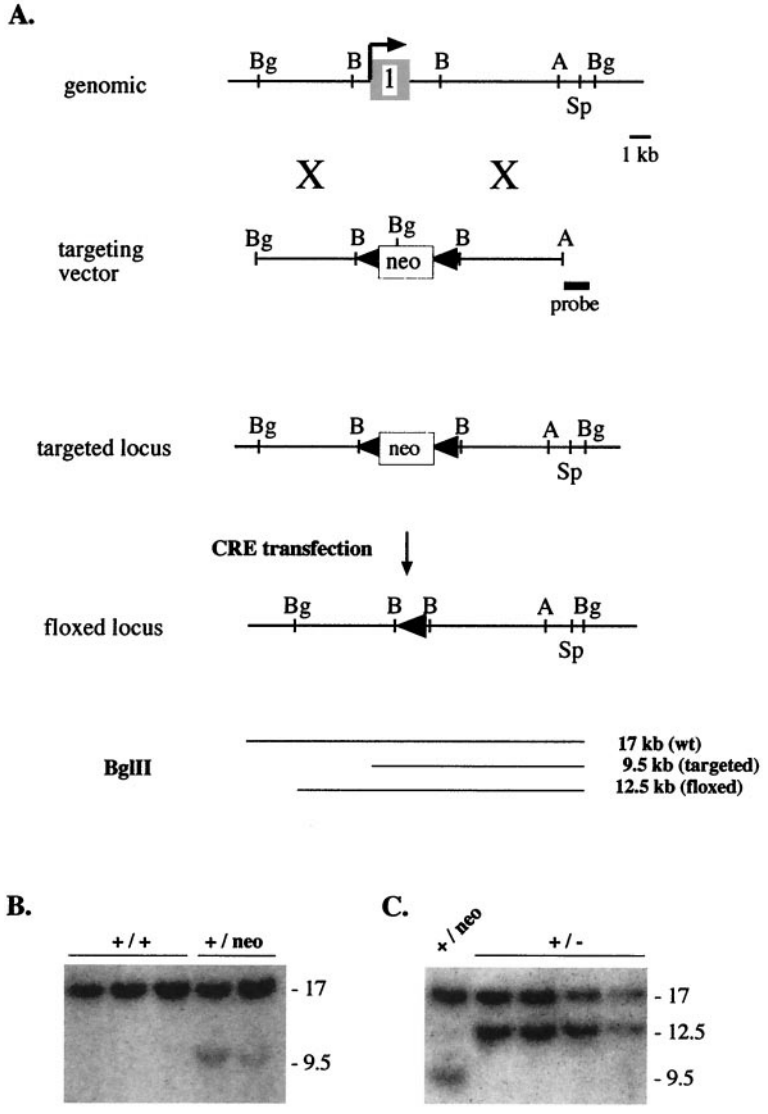

FIG. 1. Disruption of the mouse *Orct3* gene in ES cells. (A) *Orct3* gene targeting strategy. The top line is a schematic overview of the *Orct3* gene locus. Exon 1 is shown as a gray box. The arrow marks the wild-type *Orct3* promoter and the direction of transcription. Restriction enzyme sites for *Asp*718 (A), *Bam*HI (B), *Bgl*II (Bg), and *Spe*I (Sp) are indicated. In the targeting construct, a 4.3-kb *Bam*HI genomic fragment containing exon 1 was replaced by the selection cassette (neo) flanked by *loxP* sites (arrowheads). Following homologous recombination, the selection cassette was removed by CRE-mediated recombination, leaving a single *loxP* site in place of the 4.3-kb *Bam*HI fragment containing exon 1. wt, wild type. (B and C) Genotype analysis of the targeted ES cell clones (B) and the CRE-transfected ES cells (C). An 800-bp 3′ external *Asp*718-*Spe*I fragment was used as a probe on *Bgl*II-digested ES cell genomic DNA, detecting a 17-kb wild-type (+/+), a 9.5-kb homologous recombined (+/neo), and a 12.5-kb floxed (+/−) allele.

expression. To test this, RNA was isolated from various organs of adult wild-type and *Orct3* homozygous knockout mice and analyzed by Northern blotting (Fig. 2A). Wild-type mice show high expression in heart and skeletal muscle. No *Orct3* expression was detected in these tissues of homozygous mutant mice. Also, *Orct3* expression was absent in brain tissue, which shows low levels of expression in wild-type mice. In placentas of homozygous mutant embryos, no *Orct3* expression was detected at 11.5 days of gestation (Fig. 2B). At later time points, however, expression of an aberrant *Orct3* transcript was observed. Figure 2B shows expression of this aberrant transcript, which is approximately 700 bp shorter than the wild-type transcript, in 12.5- to 17.5-dpc placentas. Reverse transcription-PCR with different sets of intron-spanning *Orct3* oligonucleotide primers confirmed the presence of an *Orct3* transcript in the homozygous mutant placentas and showed that exons 3 to 11 of the *Orct3* gene were contained within this mRNA (data not shown and map in Fig. 3A). A 5′ rapid-amplification-of-cDNA-ends experiment was performed with *Orct3*-specific oligonucleotides on homozygous mutant placenta RNA. A unique 158-bp sequence that is not present in the wild-type *Orct3* transcript was identified. This sequence was mapped to intron 2 of the *Orct3* gene and contains a consensus splice donor sequence by which it splices to exon 3 of the *Orct3* gene (data not shown). The 158-bp sequence does not reintroduce an ATG translation start codon, which was removed with exon

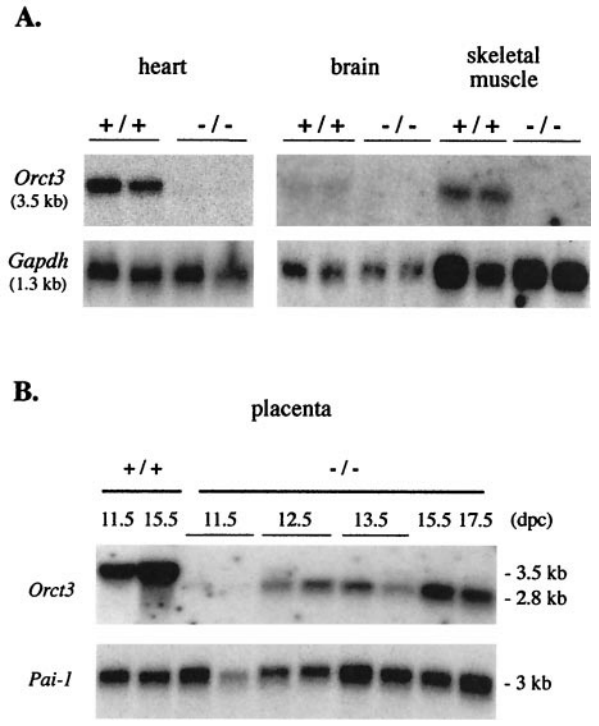

FIG. 2. Gene expression analysis in *Orct3* mutant mice. (A) Northern blot analysis of *Orct3* expression in different organs of wild-type and homozygous mutant adult mice. GAPDH was used as a loading control. (B) *Orct3* expression in wild-type and homozygous mutant mouse placentas at different stages of development. The 3.5-kb wild-type and 2.8-kb aberrant transcripts are indicated. *Pai-1* hybridization was used as a loading control.

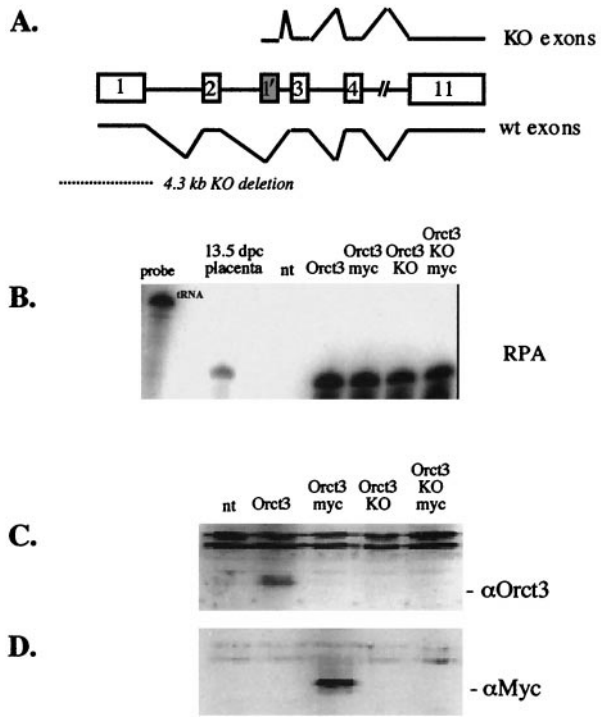

FIG. 3. The knockout (KO)-specific 2.8-kb transcript is not translated. (A) Exon map of the knockout-specific RNA 2.8-kb transcript and the wild-type (wt) mRNA. The 2.8-kb transcript lacks exons 1 and 2 but contains a novel exon (gray box labeled 1′) from intron 2 spliced onto exons 3 to 11 (there are 11 exons in wild-type *Orct3)*. The first in-frame ATG codon is within the fourth transmembrane domain, and if it were used, the predicted protein would contain only 8 of the 12 transmembrane domains of the wild-type protein. The position of the 4.3-kb deleted sequence that spans the Orct3 promoter is indicated by the dotted line. (B) RNase protection assay (RPA) of transiently transfected human embryonic kidney 293 cells. Four constructs were used: Orct3, wild-type *Orct3*/*Slc22a3* cDNA; Orct3myc, wild-type *Orct3* cDNA with a Myc tag inserted into a *Hin*dIII site located six codons before the translation stop; Orct3KO, the knockout-specific cDNA; and Orct3KOmyc, the knockout-specific cDNA containing a Myc tag inserted into a *Hin*dIII site located six codons before the translation stop. All constructs were driven by a cytomegalovirus promoter and enhancer and generated abundant RNA. 13.5 dpc, wild-type placental RNA that serves as a control for *Orct3* production; nt, nontransfected control cells. (C) Western blotting using antiserum raised to an *Orct3* peptide as described in Materials and Methods. Only the wild-type cDNA is translated; the wild-type *Orct3* Myc-tagged protein cannot be recognized by the *Orct3* antiserum, because the Myc tag is inserted in the epitope recognized by the antiserum. (D) Western blotting of the same samples using an anti-Myc antiserum; only the wild-type Myc-tagged protein is recognized.

1, into the mutant transcript. The first in-frame ATG codon is within the fourth transmembrane domain, and if it were used, the predicted protein would contain only 8 of the 12 transmembrane domains of the wild-type protein. Transient overexpression of the mutant RNA in transfected cell lines confirmed that the short transcript is incapable of generating a protein product (Fig. 3). These results show that the targeting strategy resulted in the complete absence of *Orct3* gene expression in adult mice and in early placentas, whereas at later stages in embryonic development an aberrant, noncoding *Orct3* mRNA was expressed in the placenta.

***Orct3*-null mice are viable and show no obvious phenotype.** Mice heterozygous for the two independent *Orct3* null alleles were bred to establish two independent *Orct3* knockout mouse lines that behaved similarly in all tests (see Materials and Methods). Mice homozygous for the targeted allele appeared in normal Mendelian ratios (data not shown), indicating that *Orct3* is dispensable for embryonic development. *Orct3*-null mice appear normal in stature and have a normal life span (the oldest mice in the colony are now 15 to 16 months). Both male and female *Orct3*-null mice are fertile with normal breeding behavior. In addition, female mice show normal maternal nurturing behavior and have reared the same sizes of litters as did wild-type mice. Finally, the *Orct3*-null mice show no abnormal behavior under routine housing and handling, indicating a degree of tolerance to normal stress. Histological examination of $Orct3^{-/-}$ placentas, which are the highest *Orct3*-expressing organs at any stage, and of the heart, which is the highest *Orct3*-expressing organ in adult mice, similarly revealed no cellular or structural alterations (data not shown). The heart in *Orct3*-null mice was of a normal size range, color, and appearance. In addition, the weight of the heart in *Orct3*-null mice was unchanged from that of wild-type mice (Table 1).

Impaired uptake-2 activity in adult *Orct3*-deficient mice. To study uptake-2 in *Orct3*-deficient mice, we designed a protocol measuring uptake-2-mediated accumulation of the neurotoxin MPP^+ after intravenous injection. MPP^+ has been described elsewhere as a good uptake-2 substrate and is not subject to metabolism in vivo, in contrast to the monoamines (22, 25).

TABLE 1. Weights of hearts from wild-type and *Orct3*-null adult mice aged 12 weeks

Data group no.	Heart wt (g) for sex and genotype[a]:			
	Male		Female	
	Wild type	*Orct3* KO	Wild type	*Orct3* KO
1	0.1472	0.1236	0.1316	0.1183
2	0.1638	0.1174	0.1358	0.1477
3	0.1364	0.1418	0.1138	0.1454
4	0.1886	0.1652	0.1115	0.1076
5	0.1597	0.1510	0.1240	0.1192
6	0.1512	0.1558	0.1282	0.1195
7	0.1716	0.1586	0.1502	0.1235
Mean	0.1598	0.1448	0.1279	0.1259
SD	0.0172	0.0181	0.0133	0.0149

[a] KO, knockout. For comparison of wild-type and *Orct3*-null mouse data, *P* values were 0.1376 and 0.7971 for male and female mice, respectively.

Monoamines are converted into antagonistic metabolites for uptake-2, which complicates their use as substrates in the analysis of uptake-2 activity in vivo (33). To measure a maximal effect in primary uptake, we first determined the temporal curve of [^{3}H]MPP$^+$ accumulation. Wild-type FVB/N female mice were injected intravenously with 1.0-mg/kg [^{3}H]MPP$^+$, and MPP$^+$ concentrations in the heart, liver, and plasma were determined 5, 10, 15, and 60 min after injection (Fig. 4). In both heart and liver, an increase in MPP$^+$ concentration was seen up to 15 min. At later time points, the MPP$^+$ levels decreased in both organs, following the rapid decline in MPP$^+$ plasma concentrations (Fig. 4). Based on these data in subsequent studies, the primary uptake of [^{3}H]MPP$^+$ was determined 10 min after intravenous injection.

Uptake-2 has been particularly well defined in the heart, which has high levels of *Orct3* gene expression, whereas the liver is one of the few organs that is completely lacking *Orct3* gene expression in mice. To analyze the consequences of a loss of *Orct3* for uptake-2 activity, MPP$^+$ concentrations were determined in plasma, heart, liver, and other organs of wild-type and *Orct3* mutant male and female mice (Fig. 5). In wild-type female hearts, MPP$^+$ concentrations reached 2,415 ± 331 ng/g of tissue, whereas the levels in *Orct3* mutant hearts were only 674 ± 137 ng/g (Fig. 5A). This reduction is nearly fourfold (72%) with a *P* value of <0.0001. In males, an identical reduction (72%; $P < 0.0001$) in MPP$^+$ accumulation was measured in the heart (Fig. 5B). The reduced uptake in the heart does not reflect differences in concentrations of MPP$^+$ in plasma, as those were comparable between wild-type and mutant animals (Fig. 5A and B). In the liver, no difference was found in MPP$^+$ accumulation between wild-type and *Orct3* mutant mice. As *Orct3* is not expressed in the liver, this result indicates that other systems in addition to the *Orct3* transporter mediate MPP$^+$ uptake and that the activity of these systems is not affected by a deletion of *Orct3* (Fig. 5A and B). A total of 12 additional organs of wild-type and *Orct3* mutant mice were analyzed for a difference in MPP$^+$ uptake (Fig. 5C and D). A similar distribution of MPP$^+$ was seen in males and females, with some sex-specific differences in adrenal glands and skeletal muscle. The highest accumulation was detected in adrenal glands, and only very low MPP$^+$ concentrations were measured in the brain, which is due to the inability of MPP$^+$ to cross the blood-brain barrier (29). Taken together, these data show that in adult mice *Orct3* deficiency results in a specific impairment of uptake-2 activity in the heart.

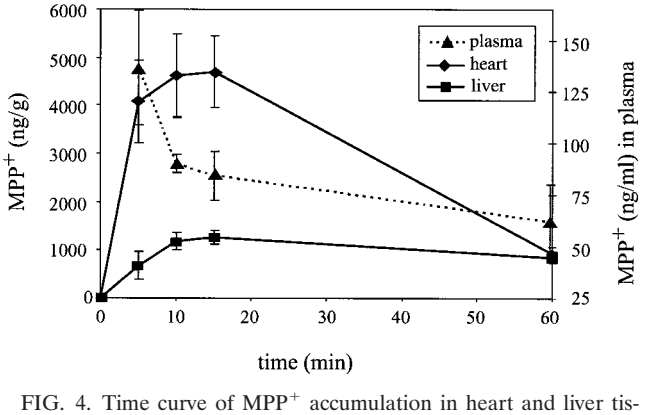

FIG. 4. Time curve of MPP$^+$ accumulation in heart and liver tissues of wild-type female mice. Levels of MPP$^+$ in the heart (♦) and liver (■) (plotted on the primary *y* axis in nanograms per gram of tissue) are indicated at different time points after intravenous injection. The MPP$^+$ plasma levels are shown by the dashed line (▲) and plotted on the secondary *y* axis in nanograms per milliliter.

Orct3 transports MPP$^+$ at the fetoplacental interface. We next addressed the role of *Orct3* in the placenta. Pregnant females of an *Orct3* heterozygous cross were injected at 15.5 dpc with 1.0 mg of [^{3}H]MPP$^+$ per kg. The MPP$^+$ concentrations were determined in embryos, placentas, and amniotic fluid 10 min after injection (Fig. 6). The highest levels of MPP$^+$ were detected in the placenta, intermediate levels were detected in the embryo, and the lowest levels were detected in the amniotic fluid. In embryos, a threefold reduction in MPP$^+$ accumulation, from 64.7 ± 22.7 ng/g in wild-type mice to 20.4 ± 4.4 ng/g in mutants, was detected ($P < 0.001$). However, no differences in [^{3}H]MPP$^+$ accumulation were found in placentas and amniotic fluid of both groups. Since *Orct3* is not expressed in embryonic tissue, these data indicate that *Orct3* is the rate-limiting step in MPP$^+$ transport from the placenta to the fetus but does not play a major role in placental uptake from the maternal circulation. These results identify the placenta as a novel uptake-2 site of action.

Noradrenaline and dopamine levels in *Orct3*-null mice. Embryos and placentas at 12.5 dpc with a wild-type and an *Orct3*-null genotype were obtained from a heterozygous mating. Noradrenaline and dopamine steady-state levels were measured by HPLC. Table 2 shows that, although both noradrenaline and dopamine levels are reduced by approximately 50% in *Orct3*-null embryos, the results are not statistically significant ($P = 0.1015$). Samples with the same genotype and obtained from the same litter showed a very large variation in noradrenaline and dopamine steady-state levels for which there is no current explanation. An independent examination of monoamine levels in heart tissue has also found a large variation among animals with the same genotype, with no significant difference between wild-type and *Orct3*-null mice (B. Giros and S. Gautron, personal communication)

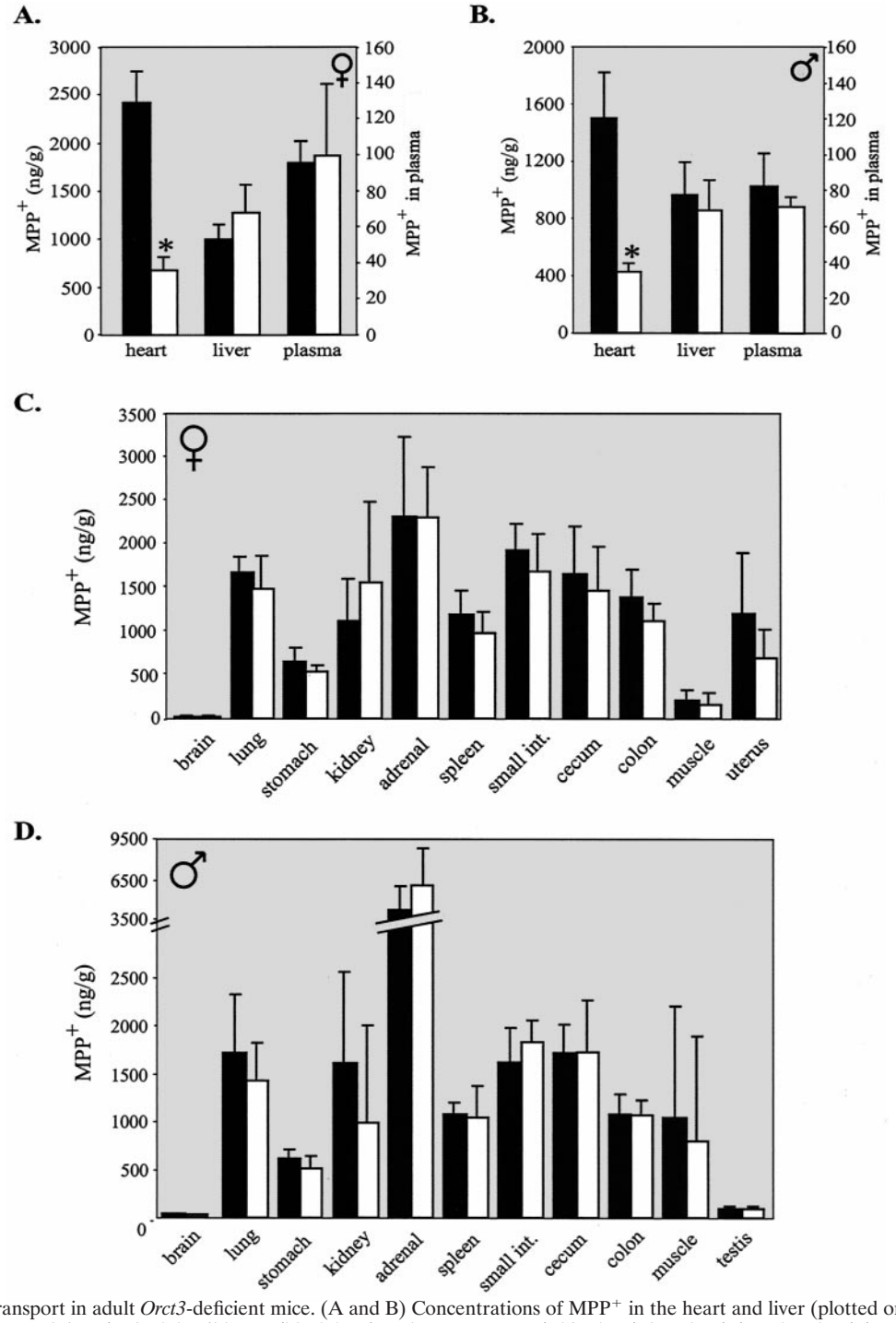

FIG. 5. MPP^+ transport in adult *Orct3*-deficient mice. (A and B) Concentrations of MPP^+ in the heart and liver (plotted on the primary *y* axis in nanograms per gram of tissue) of adult wild-type (black bars) and *Orct3* mutant (white bars) females (A) and males (B). The levels in plasma are also shown and are plotted on the secondary *y* axis in nanograms per milliliter. The asterisk indicates a statistically significant difference. *P* values were <0.0001 for both male and female hearts. (C and D) MPP^+ distribution in different organs of adult wild-type (black bars) and *Orct3* mutant (white bars) female (C) and male (D) mice. small int., small intestine.

DISCUSSION

In this report, we have described the targeted inactivation of the mouse extraneuronal monoamine transporter gene *Orct3*, which has been shown to function as uptake-2. Removal of exon 1 abolished transcription in tissues of adult mice but resulted in an aberrant noncoding transcript in the placenta. We have analyzed uptake-2 activity in *Orct3*-null mice using the neurotoxin MPP^+ as a substrate and identified a transport phenotype in the adult heart and in the embryonic placenta. Despite the large differences in MPP^+ transport in embryos

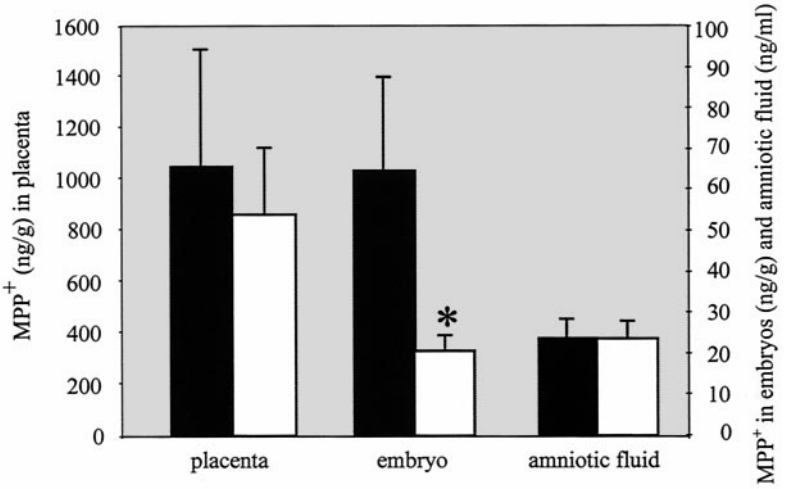

FIG. 6. Placental MPP^+ transport. MPP^+ distribution in wild-type (black bars) and *Orct3* mutant (white bars) placentas (plotted on the primary *y* axis) and embryos and amniotic fluid (plotted on the secondary *y* axis). The asterisk indicates a statistically significant difference. The *P* value was <0.001 for embryos.

and adult hearts, an overt physiological or neural phenotype in *Orct3* mutant mice that may be associated with altered extracellular monoamine concentrations was not observed. In addition, no significant differences in the steady-state levels of noradrenaline and dopamine could be detected in either embryos or placentas.

Targeted inactivation of the *Orct3* gene was performed by deletion of a 4.3-kb genomic fragment that contains the *Orct3* gene promoter and exon 1. The *Orct3* promoter consists of two closely linked transcriptional start sites that were mapped 150 and 170 bp upstream of the beginning of the CpG island in which exon 1 is embedded and were fully removed by the deletion (data not shown). *Orct3* expression was completely abolished in all tissues of adult homozygous mutant mice. Later-stage placentas from 12.5 dpc to term, however, express an aberrant, noncoding transcript. This transcript is not driven by the wild-type *Orct3* gene promoter, as it was fully included in the targeted deletion. These data indicate that deletion of the wild-type transcriptional start sites activated an ectopic promoter sequence to drive expression of the aberrant transcript. Alternatively, deletion of the wild-type promoter may have fortuitously joined together a DNA sequence that can drive expression of the aberrant transcript. The expression, however, of the aberrant nontranslated transcript is tissue specific and temporally restricted in development.

To study the role of *Orct3* in uptake-2 function in vivo, we performed transport studies using the neurotoxin MPP^+ as a substrate. MPP^+ has been described elsewhere in the etiology of 1,2,3,6-methylphenyltetrahydropyridine (MPTP)-induced Parkinson's disease (reviewed in reference 10). To exert its neurotoxic effect on the central catecholaminergic neurons, MPTP requires conversion to MPP^+ by monoamine oxidase B (Maob) in glial cells. Subsequently, MPP^+ has to leave the glial cells, upon which it is transported into the catecholaminergic

TABLE 2. HPLC analysis of noradrenaline and dopamine levels in 12.5-dpc embryonic and placental tissues[a]

Data group no.	Level of monoamine (ng [embryo] or pg [placenta]/mg of protein) for sample type and genotype							
	Embryo				Placenta			
	Noradrenaline		Dopamine		Noradrenaline		Dopamine	
	WT	KO	WT	KO	WT	KO	WT	KO
1	26.58	33.95	1.13	2.00	517.37	149.30	70.44	35.14
2	34.68	24.72	1.79	1.24	166.97	144.15	35.65	30.04
3	12.78	20.04	0.82	0.98	101.67	119.90	26.03	26.88
4	72.58	43.62	4.01	2.18	162.72	80.69	40.95	28.96
5	177.04	20.94	10.81	1.39	182.39	433.78	43.34	76.34
6	157.85	79.64	8.70	4.70	227.60	230.92	41.50	44.37
7	33.56	62.67	1.63	5.34	125.52	172.90	29.29	45.44
8	157.22	30.33	7.00	1.84	136.79	102.06	40.64	20.25
Mean	84.04	39.49	4.49	2.46	202.63	179.21	40.98	38.30
SD	68.61	21.45	3.86	1.64	132.79	112.64	13.43	17.24

[a] Eight embryos and placentas for each genotype were analyzed, and a two-tailed unpaired Student *t* test was applied to the data. KO, knockout; WT, wild type. *P* values for the wild-type mice compared with knockout mice were as follows: embryos, 0.1015 and 0.1933, and placentas, 0.7094 and 0.7341, for noradrenaline and dopamine, respectively.

neurons by the neuronal dopamine uptake system. Previously, it has been shown by in vitro cell culture that MPP^+ is able to make use of the extraneuronal monoamine transport system to exit human glial cells (24). In this report, we have shown that Orct3 transports MPP^+ in vivo in mice, raising the possibility that *Orct3* is an important mediator of MPTP neurotoxicity. In addition to the effect in the central nervous system, it has been reported that systemic injection of MPP^+ or MPTP results in severe depletion of heart noradrenaline concentrations (12). The cardiac depletion is resistant to desipramine and GBR12909, suggesting that there is no involvement of the uptake-1 transporters Net and Dat (13, 20). Our transport studies show reduced MPP^+ uptake in hearts of *Orct3*-deficient mice, which suggests that *Orct3* might be involved in the action of MPP^+-MPTP-mediated depletion of cardiac noradrenaline.

Uptake-2 has been identified in various organs, like the heart and uterus. Both organs express high levels of *Orct3*. However, our results identified a major effect of *Orct3* deficiency on MPP^+ uptake in only adult hearts. MPP^+ accumulation was reduced by 72% in *Orct3* mutant hearts in males and females. This reduction is identical, despite the fact that nearly twofold-lower levels of MPP^+ were measured in wild-type males than in the females (Fig. 5A and B). This indicates that the relative contribution of uptake-2 in MPP^+ transport is not different between males and females. A second difference in the amount of MPP^+ accumulation was found in hearts of inbred FVB/N females and wild-type females of a mixed genetic background (Fig. 4 and 5A). The difference in MPP^+ accumulation might be explained by a differential contribution of different genetic backgrounds. However, there is also an age difference between the two cohorts (7 and 12 weeks, respectively), which may be an important contributor. In the uterus, a nearly twofold reduction in MPP^+ accumulation was observed between wild-type and *Orct3*$^{-/-}$ females, but this was not statistically significant (Fig. 5C). In pigs, it was demonstrated that uptake-1 and uptake-2 activity in the uterine artery vary during the estrous cycle (7). Since the mice in our experiments were not synchronized, this could explain the large variation seen for the uterus that may potentially mask an effect of *Orct3* deficiency. Other *Orct3*-expressing organs showed no difference in MPP^+ uptake. This might be caused by a functional redundancy with other transporter genes. *Orct3* is only moderately expressed in the kidney, for instance, whereas the closely related organic cation transporter gene *Orct2* is found at high levels (21). As *Orct2* is also capable of MPP^+ transport, expression of this gene could contribute significantly to the total MPP^+ accumulation in the kidney (17). Similarly, the *Orct1* gene is highly expressed in the liver, which may account for the MPP^+ uptake measured in this tissue (Fig. 4 and 5).

The placental MPP^+ transport studies show that Orct3 transports MPP^+ between the placenta and fetus, but not to the maternal circulation, and identify the placenta as a novel uptake-2 site of action (Fig. 6). It has been reported previously that during development embryos show a high monoamine turnover compared with any other physiological condition seen for adults (30). For sheep, it has been determined that nearly 50% of the total in utero monoamine clearance was mediated by the placenta. Only part of the placental activity was assigned to the action of neuronal monoamine transporters, as was determined by inhibition mediated by cocaine, which is a neuronal monoamine transporter antagonist (5). Using RNA in situ hybridization, we have recently described the cellular expression pattern of *Orct3* and the monoamine-degrading enzyme gene *Maoa* in the mouse placenta. The two genes are expressed in a similar pattern in the labyrinth layer (34), indicating that they could form a functional monoamine degradation pathway. This interpretation is supported by the transport studies presented here that have identified an *Orct3*-mediated uptake-2 activity at the fetoplacental interface.

The MPP^+ transport studies show that *Orct3* is an essential component in vivo for the transport activity of the extraneuronal monoamine clearance system known as uptake-2. Transport defects in *Orct3*-deficient mice were observed in embryonic development. However, despite a broad expression pattern in adult animals, an essential function is seen in only one adult organ, the heart. Surprisingly, despite significant differences in MPP^+ uptake, the *Orct3*-null mice show no overt neural or physiological dysfunction as embryos or adults that may indicate a monoamine imbalance. In addition, we have been unable to identify a significant difference in the levels of two tested monoamines in *Orct3*-null embryos that show a 65% reduction in MPP^+ levels. Thus, the functional significance of the role of the *Orct3* gene in monoamine transport remains unclear. These results do not dismiss a function for the *Orct3* gene in extraneural monoamine transport, but they indicate the possibility that its role is more complex than has been predicted.

ACKNOWLEDGMENTS

R. Zwart and S. Verhaagh contributed equally to this work.

We thank C. Brouwer and J. Vink for help with the ES cell work in the gene targeting experiment. K. van Veen is acknowledged for the blastocyst injections, N. Bosnie and T. Maidment are acknowledged for taking good care of the mice, and J. W. Jonker is acknowledged for help with the MPP^+ transport studies. We thank B. Giros and S. Gautron for sharing their unpublished data; A. H. Schinkel, J. W. Jonker, and all members of the lab for critical discussions and reading of the manuscript; and A. Berns for constant help and support.

This work was supported by a grant from the Dutch Cancer Society.

REFERENCES

1. **Amara, S. G., and M. J. Kuhar.** 1993. Neurotransmitter transporters: recent progress. Annu. Rev. Neurosci. **16:**73–93.
2. **Auffray, C., and F. Rougeon.** 1980. Purification of mouse immunoglobulin heavy-chain messenger RNAs from total myeloma tumor RNA. Eur. J. Biochem. **107:**303–314.
3. **Bengel, D., D. L. Murphy, A. M. Andrews, C. H. Wichems, D. Feltner, A. Heils, R. Mossner, H. Westphal, and K. P. Lesch.** 1998. Altered brain serotonin homeostasis and locomotor insensitivity to 3, 4-methylenedioxymethamphetamine ("Ecstasy") in serotonin transporter-deficient mice. Mol. Pharmacol. **53:**649–655.
4. **Breidert, T., F. Spitzenberger, D. Grundemann, and E. Schomig.** 1998. Catecholamine transport by the organic cation transporter type 1 (OCT1). Br. J. Pharmacol. **125:**218–224.
5. **Bzoskie, I., I. Blount, K. Kashiwai, J. Humme, and J. F. Padbury.** 1997. Placental norepinephrine transporter development in the ovine fetus. Placenta **18:**65–70.
6. **Church, G. M., and W. Gilbert.** 1984. Genomic sequencing. Proc. Natl. Acad. Sci. USA **81:**1991–1995.
7. **Dynarowicz, I., T. Trapkowski, and T. Pirus.** 1993. Uptake-1, Uptake-2 and the release of [3H]-noradrenaline in uterine artery of pigs during the oestrous cycle. Arch. Vet. Pol. **33:**259–267.
8. **Eisenhofer, G., R. McCarty, K. Pacak, H. Russ, and E. Schomig.** 1996. Disprocynium24, a novel inhibitor of the extraneuronal monoamine transporter, has potent effects on the inactivation of circulating noradrenaline and adrenaline in conscious rat. Naunyn-Schmiedeberg's Arch. Pharmacol. **354:** 287–294.

9. **Fassler, R., and M. Meyer.** 1995. Consequences of lack of beta 1 integrin gene expression in mice. Genes Dev. **9:**1896–1908.
10. **Feldman, R. S., J. S. Meyer, and L. F. Quenzer.** 1997. Principles of neuropsychopharmacology. Sinauer Associates Inc., Sunderland, Mass.
11. **Friedgen, B., R. Wolfel, H. Russ, E. Schomig, and K. H. Graefe.** 1996. The role of extraneuronal amine transport systems for the removal of extracellular catecholamines in the rabbit. Naunyn-Schmiedeberg's Arch. Pharmacol. **354:**275–286.
12. **Fuller, R. W., and S. K. Hemrick-Luecke.** 1986. Depletion of norepinephrine in mouse heart by 1-methyl-4-phenyl-1,2,3,6-tetrahydropyridine (MPTP) mimicked by 1-methyl-4-phenylpyridinium (MPP+) and not blocked by deprenyl. Life Sci. **39:**1645–1650.
13. **Fuller, R. W., S. K. Hemrick-Luecke, and D. W. Robertson.** 1988. Comparison of 1-methyl-4-phenyl-1,2,3,6-tetrahydropyridine (MPTP) and 1-methyl-4-phenylpyridinium (MPP+) effects on mouse heart norepinephrine. Biochem. Pharmacol. **37:**3343–3347.
14. **Giros, B., M. Jaber, S. R. Jones, R. M. Wightman, and M. G. Caron.** 1996. Hyperlocomotion and indifference to cocaine and amphetamine in mice lacking the dopamine transporter. Nature **379:**606–612.
15. **Grundemann, D., J. Babin-Ebell, F. Martel, N. Ording, A. Schmidt, and E. Schomig.** 1997. Primary structure and functional expression of the apical organic cation transporter from kidney epithelial LLC-PK1 cells. J. Biol. Chem. **272:**10408–10413.
16. **Grundemann, D., S. Koster, N. Kiefer, T. Breidert, M. Engelhardt, F. Spitzenberger, N. Obermuller, and E. Schomig.** 1998. Transport of monoamine transmitters by the organic cation transporter type 2, OCT2. J. Biol. Chem. **273:**30915–30920.
17. **Grundemann, D., G. Liebich, N. Kiefer, S. Koster, and E. Schomig.** 1999. Selective substrates for non-neuronal monoamine transporters. Mol. Pharmacol. **56:**1–10.
18. **Grundemann, D., B. Schechinger, G. A. Rappold, and E. Schomig.** 1998. Molecular identification of the corticosterone-sensitive extraneuronal catecholamine transporter. Nat. Neurosci. **1:**349–351.
19. **Iversen, L. L.** 1965. The uptake of catechol amines at high perfusion concentrations in the rat isolated heart: a novel catechol amine uptake process. Br. J. Pharmacol. **25:**18–33.
20. **Kujacic, M., and A. Carlsson.** 1994. Effects of MPP+ on catecholamine levels in adrenal glands and heart of rats. Naunyn-Schmiedeberg's Arch. Pharmacol. **350:**245–251.
21. **Mooslehner, K. A., and N. D. Allen.** 1999. Cloning of the mouse organic cation transporter 2 gene, Slc22a2, from an enhancer-trap transgene integration locus. Mamm. Genome **10:**218–224.
22. **Russ, H., M. Gliese, J. Sonna, and E. Schomig.** 1992. The extraneuronal transport mechanism for noradrenaline (Uptake-2) avidly transports 1-methyl-4-phenylpyridinium (MPP+). Naunyn-Schmiedeberg's Arch. Pharmacol. **346:**158–165.
23. **Russ, H., J. Sonna, K. Keppler, S. Baunach, and E. Schomig.** 1993. Cyanine-related compounds: a novel class of potent inhibitors of extraneuronal noradrenaline transport. Naunyn-Schmiedeberg's Arch. Pharmacol. **348:**458–465.
24. **Russ, H., K. Staust, F. Martel, M. Gliese, and E. Schomig.** 1996. The extraneuronal transporter for monoamine transmitters exists in cells derived from human central nervous system glia. Eur. J. Neurosci. **8:**1256–1264.
25. **Sayre, L. M.** 1989. Biochemical mechanism of action of the dopaminergic neurotoxin 1-methyl-4-phenyl-1,2,3,6-tetrahydropyridine (MPTP). Toxicol. Lett. **48:**121–149.
26. **Schomig, E., and C. L. Schonfeld.** 1990. Extraneuronal noradrenaline transport (Uptake-2) in a human cell line (Caki-1 cells). Naunyn-Schmiedeberg's Arch. Pharmacol. **341:**404–410.
27. **Schweifer, N., and D. P. Barlow.** 1996. The Lx1 gene maps to mouse chromosome 17 and codes for a protein that is homologous to glucose and polyspecific transmembrane transporters. Mamm. Genome **7:**735–740.
28. **Shannon, J. R., N. L. Flattem, J. Jordan, G. Jacob, B. K. Black, I. Biaggioni, R. D. Blakely, and D. Robertson.** 2000. Orthostatic intolerance and tachycardia associated with norepinephrine-transporter deficiency. N. Engl. J. Med. **342:**541–549.
29. **Snijder, S. H., R. J. D'Amato, J. S. Nye, and J. A. Javitch.** 1986. Selective uptake of MPP+ by dopamine neurons is required for MPTP neurotoxicity: studies in brain synaptosomes and PC-12 cells, p. 191–201. *In* S. P. Markey, N. Castagnoli, A. J. Trevor, and I. J. Kopin (ed.), MPTP: a neurotoxin producing a Parkinsonian syndrome. Academic Press, Inc., Orlando, Fla.
30. **Stein, H., K. Oyama, A. Martinez, B. Chappell, and J. Padbury.** 1993. Plasma epinephrine appearance and clearance rates in fetal and newborn sheep. Am. J. Physiol. **265:**R756–R760.
31. **Streich, S., M. Bruss, and H. Bonisch.** 1996. Expression of the extraneuronal monoamine transporter (Uptake-2) in human glioma cells. Naunyn-Schmiedeberg's Arch. Pharmacol. **353:**328–333.
32. **Thomas, S. A., A. M. Matsumoto, and R. D. Palmiter.** 1995. Noradrenaline is essential for mouse fetal development. Nature **374:**643–646.
33. **Trendelenburg, U.** 1988. The extraneuronal uptake and metabolism of catecholamines. Handb. Exp. Pharmacol. **90/I:**279–319.
34. **Verhaagh, S., D. P. Barlow, and R. Zwart.** 2001. The extraneuronal monoamine transporter Slc22a3/Orct3 co-localizes with the Maoa metabolizing enzyme in mouse placenta. Mech. Dev. **100:**127–130.
35. **Verhaagh, S., N. Schweifer, D. P. Barlow, and R. Zwart.** 1999. Cloning of the mouse and human solute carrier 22a3 (Slc22a3/SLC22A3) identifies a conserved cluster of three organic cation transporters on mouse chromosome 17 and human 6q26–q27. Genomics **55:**209–218.
36. **Wu, X., R. Kekuda, W. Huang, Y. J. Fei, F. H. Leibach, J. Chen, S. J. Conway, and V. Ganapathy.** 1998. Identity of the organic cation transporter OCT3 as the extraneuronal monoamine transporter (Uptake-2) and evidence for the expression of the transporter in the brain. J. Biol. Chem. **273:**32776–32786.
37. **Xu, F., R. R. Gainetdinov, W. C. Wetsel, S. R. Jones, L. M. Bohn, G. W. Miller, Y. M. Wang, and M. G. Caron.** 2000. Mice lacking the norepinephrine transporter are supersensitive to psychostimulants. Nat. Neurosci. **3:**465–471.
38. **Zwart, R., S. Verhaagh, J. de Jong, M. Lyon, and D. P. Barlow.** Genetic analysis of the organic cation transporter genes *Orct2*/*Slc22a2* and *Orct3Slc22a3* reduces the critical region for the *t* haplotype mutant t^{w73} to 200 kb. Mammal. Genome, in press.